CHEMISTRY OF MATERIALS

Article

pubs.acs.org/cm

Quantitative Dedoping of Conductive Polymers

Ian E. Jacobs,[†] Faustine Wang,[‡] Nema Hafezi,[∥] Cristina Medina-Plaza,[‡,§] Thomas F. Harrelson,[‡] Jun Li,[‡] Matthew P. Augustine,[∥] Mark Mascal,[∥] and Adam J. Moulé*[,‡,∥]

[†]Department of Materials Science, [‡]Department of Chemical Engineering, and [∥]Department of Chemistry, University of California, Davis, California 95616, United States

[§]Department of Inorganic Chemistry, Engineers School, University of Valladolid, 47002 Valladolid, Spain

Supporting Information

ABSTRACT: Although doping is a cornerstone of the inorganic semiconductor industry, most devices using organic semiconductors (OSCs) make use of intrinsic (undoped) materials. Recent work on OSC doping has focused on the use of dopants to modify a material's physical properties, such as solubility, in addition to electronic and optical properties. However, if these effects are to be exploited in device manufacturing, a method for dedoping organic semiconductors is required. Here, we outline two chemical strategies for dedoping OSC films. In the first strategy, we use an electron donor (a tertiary amine) to act as competitive donor. This process is based on a thermodynamic equilibrium between ionization of the donor and OSC and results in only partial dedoping. In the second strategy, we use an electron donor that subsequently reacts with the p-type dopant to create a nondoping product molecule. Primary and secondary amines undergo a rapid addition reaction with the dopant molecule 2,3,5,6-tetrafluoro-7,7,8,8,-tetracyanoquinodimethane (F4TCNQ), with primary amines undergoing a further reaction eliminating HCN. Under optimized conditions, films of semiconducting polymer poly(3-hexylthiophene) (P3HT) dedoped with 1-propylamine (PA) reach as-cast fluorescence intensities within 5 s of exposure to the amine, eventually reaching 140% of the as-cast values. Field-effect mobilities similarly recover after dedoping. Quantitative fluorescence recovery is possible even in highly fluorescent polymers such as PFB, which are expected to be much more sensitive to residual dopants. Interestingly, treatment of undoped films with PA also yields increased fluorescence intensity and a reduction in conductivity of at least 2 orders of magnitude. These results indicate that the process quantitatively removes not only F4TCNQ but also intrinsic p-type impurities present in as-cast films. The dedoping strategies outlined in this article are generally applicable to other p- and n-type molecular dopants in OSC films.

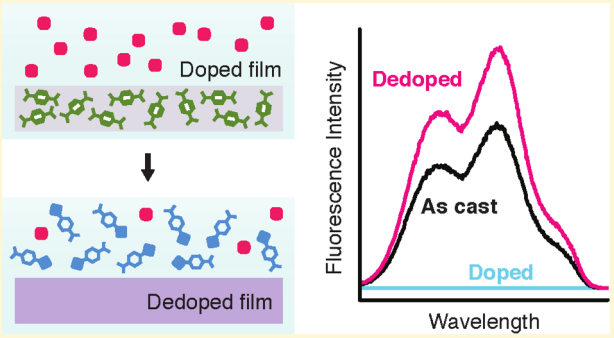

INTRODUCTION

In recent decades, as electronics have found their way into an increasing range of consumer products, there has been growing demand for cheaper devices in more flexible form factors. A leading class of materials in this field are organic semiconductors (OSCs). Although OSCs are unlikely to replace silicon in very large scale integrated (VLSI) circuit applications,[1] they are cheap and flexible, can be chemically tailored to specific applications, and can be deposited from solution over large areas at very low cost.[2] These features make OSCs especially promising in applications such as flexible displays,[3] "artificial skin" sensor arrays,[4] and photovoltaics.[5,6]

Trace impurities can have drastic effects on the electronic and optical properties of semiconductors. The intentional addition of these impurities, called doping, underlies many fundamental electronic devices such as transistors, diodes, LEDs, and photovoltaics.[7] Dopants either donate electrons to the conduction band (n-type doping) or accept electrons from the valence band (p-type doping), shifting the Fermi level and increasing the number of free charge carriers in the lattice. In a p-type doped semiconductor, the number of free holes p_{free} and bound (immobile) holes p_{bound} together comprise the uncompensated charge density: $p_{unc} = p_{free} + p_{bound}$.[8] In inorganic semiconductors, dopant atoms substitute for those of the semiconductor. Doped semiconductors are fabricated by diffusion of suitable donor or acceptor species from an interface or by ion implantation.[7] These processes are irreversible, but it is still possible to reduce the effective doping level in a particular region by adding dopants of opposite polarity (i.e., n-type). This approach, called compensation doping, results in a reduction of p_{unc} but always increases the total charge density, $p_{comp} = n_{comp}$, since the ionized p- and n-type dopants remain in the material. In inorganics, generally all dopants are ionized and result in free charge carriers at room temperature (that is, $p_{bound} \approx 0$), so only ppm−ppt doping levels are needed in typical applications.[7] Therefore, even in compensated materials the

Received: November 16, 2016
Revised: December 27, 2016
Published: December 30, 2016

DOI: 10.1021/acs.chemmater.6b04880
Chem. Mater. 2017, 29, 832−841

total charge density can be kept quite low, making compensation doping a practical approach to fabricating homojunctions.

Doping is superficially similar in OSCs, except that the dopant species are molecular rather than atomic. However, in part due to their much lower dielectric constants, OSCs show very low doping efficiencies. A well studied organic semiconductor:dopant system is poly(3-hexylthiophene) (P3HT) doped with 2,3,5,6-tetrafluoro-7,7,8,8,-tetracyanoquinodimethane (F4TCNQ).[9−19] In P3HT:F4TCNQ, for reasons not yet fully understood, only about 5% of the holes injected by dopants actively contribute to charge transport[9] (that is, $p_{free} \ll p_{bound}$), even though nearly all F4TCNQ molecules in the film are fully ionized.[15] Therefore, relevant doping levels in OSCs are much higher, ranging from ppt to well over 100 wt % in commercial formulations of PEDOT:PSS (poly(3,4-ethylenedioxythiophene)polystyrenesulfonate), another widely used polymer:dopant blend. Clearly, with such high doping levels required, compensation doping is not a feasible approach to fabricating homojunctions in organic semiconductors.

Fortunately, the ability to solution process and perform chemistry on dopant molecules affords the opportunity to reduce both doping levels *and* compensated charge density by direct removal of dopants from OSC films. This processing pathway is not possible for inorganic semiconductors. Partially reversible doping has been demonstrated previously by exposure of doped films to air or polar solvents,[20] by heating,[17,18] and by using acid−base chemistry in protic polymers such as polyaniline.[21−24] However, doping induced polarons are extremely efficient exciton quenchers and even relatively dilute concentrations of dopants can have major impacts on photoluminescence efficiency,[8] so a method to enable quantitative removal of dopants would be very valuable.

Doping can play an additional, somewhat unexpected role in organic semiconductor device manufacturing. In recent work, it was demonstrated that p-type doping acts as a "solubility switch," rendering some conductive polymers insoluble without cross-linking or otherwise structurally altering the material.[18] By selectively adding or removing dopants from films, solubility contrast is generated, allowing for subdiffraction limited optical patterning[25] and layering of mutually soluble materials.[18] We call this process doping-induced solubility control (DISC).[18,19,25,26] However, in many device applications intrinsic (undoped) material properties are required; therefore, the ability to quantitatively dedope films after patterning or layering is of paramount importance. In previous work,[18] we found that when undoped P3HT films were doped with F4TCNQ and then dedoped with a 9:1 mixture of acetone:ethylenediamine at 60 °C, the dedoped film's optical, electrical, and chemical properties returned almost exactly to their as-cast values.[18]

In this work, we explore the mechanisms by which quantitative dedoping of P3HT:F4TCNQ can be accomplished and optimize the dedoping process. Under optimized conditions, we are able to obtain fluorescence intensities even greater than as-cast, corresponding to free carrier densities lower than as-cast films, after only a five second soak in a room temperature 1-propylamine (PA) dedoping solution. In addition, it was found that soaking as-cast (undoped) films in PA solutions similarly increased film fluorescence intensity and decreased conductivity, indicating these solutions remove intrinsic p-type defects. This approach to dedoping, along with other aspects of DISC, has the potential to simplify the solution-based manufacture of complex devices.

Approaches to Dedoping. In organic electronics, p-type dopants take the form of strong electron acceptors, which are capable of undergoing ground state charge transfer with the organic semiconductor.[28] In some cases, the reaction between semiconductor and dopant results in the evolution of a gas, rendering the process irreversible.[29,30] Irreversible reactions are not amenable to dedoping, so for obvious reasons we restrict the present study to simple, single-electron transfer p-type doping. Here, the dopant electron affinity (EA) must be greater than the semiconductor ionization energy (IE), as is the case for P3HT:F4TCNQ. However, it should be noted that the formation of a charge transfer complex involving fractional charge transfer between the dopant and semiconductor can result even when the dopant EA is lower than the IE of the OSC.[31−33] An energy level diagram of P3HT and F4TCNQ before charge transfer is shown in Figure 1a. Figure 1b shows the energy levels of P3HT and F4TCNQ after charge transfer using the model developed by Winkler et al., assuming that the charges are sufficiently separated such that they can be considered noninteracting.[27] In both the dopant and the polymer, on-site interactions split the singly occupied orbitals into two sub-bands.[27,33,34] The occupied sub-band shifts below the energy of the neutral HOMO, while the unoccupied band moves into the band gap.

The simplest approach to dedoping, competitive dedoping, is shown in Figure 1c. In this process, the doped film is immersed in a solution containing a donor molecule with an IE low enough to transfer charge to the unoccupied midgap state of the polymer, mixed with a polar solvent capable of dissolving the ionized dopant but not the polymer. Charge transfer from the donor reduces the polymer to its neutral state, thus dedoping it. Sufficiently strong donors could also further reduce the dopant, although this should not affect the dedoping process. In either case, the ionized dopant then dissolves to compensate the positively charged donor molecules in solution, as shown schematically in Figure 1d. With competitive dedoping, the amount of residual dopant in the film will be primarily controlled by the energy level difference between the polymer and the donor HOMOs. Since this is an equilibrium process and the donor strength is limited by the condition that it must not be capable of reducing the polymer, e.g., P3HT to $P3HT^{\bullet-}$, this process is not expected to ever achieve complete dedoping.

A more sophisticated approach—reactive dedoping—is shown in Figure 1e. The film is again immersed in an orthogonal solvent, this time containing a donor reactive toward the dopant but nonreactive toward the polymer. The process begins identically to competitive dedoping, with charge transfer from the donor to the polymer reducing the polymer to its undoped state and the ionized dopant dissolving into solution (Figure 1c,d). The ionized dopant and donor then react to form a nondoping product. Such reactions would be expected to proceed through a charge transfer complex intermediate.[35] However, even if the reaction goes through a neutral intermediate or if the donor is not strong enough to reduce the polymer, thermal fluctuations could transiently transfer charge back from the ionized dopant to the ionized donor. In either case, since the driving force for solvation of F4TCNQ in P3HT is ionization and charge screening,[19] after reaction the product should prefer to dissolve in the solvent

DOI: 10.1021/acs.chemmater.6b04880
Chem. Mater. 2017, 29, 832−841

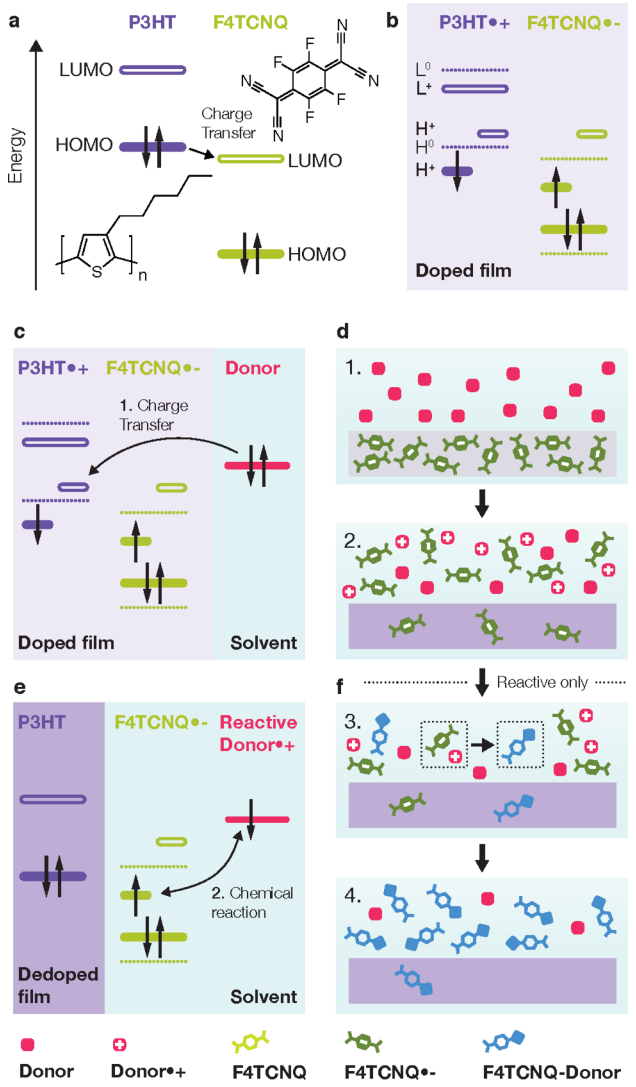

Figure 1. (a) Schematic energy level diagram showing P3HT and F4TCNQ HOMO and LUMO levels before charge transfer. (b) Energy levels after charge transfer, showing the polaron states (L^+, H^+) relative to the neutral states (L^0, H^0).[27] (c) Both competitive and reactive dedoping begin with charge transfer from the donor to the polymer. (d) Schematic illustrating the dedoping process. 1. Donor is introduced, reducing the film to its undoped state. 2. Most of the dopant dissolves, but remains ionized. (e) Reactive doping continues from the same initial steps as competitive doping (c, d), but after dissolution, the dopant reacts with the donor to form a nondoping product. (f) Schematic illustrating reactive dedoping, continuing from (d): 3. The donor and dopant react to form a nondoping product. 4. The reaction proceeds to completion, passivating any remaining dopants.

rather than remain in the film. A schematic of the process is shown in Figure 1d,f.

The reactive doping approach has two distinct advantages over competitive dedoping. First, the amount of residual dopant in the film is controlled by the reaction equilibrium constant, rather than the relative donor strengths. The reaction equilibrium constant can be extremely large assuming the back-reaction rate is slow, which would be expected for a strongly exergonic reaction. Fortunately, since dopant molecules by design are strongly electrophilic (p-type dopants) or nucleophilic (n-type dopants), in general there should be a range of highly exothermic reactions in which these molecules can participate. Second, assuming that the reaction proceeds to completion, any residual dopant that might remain in the film will be passivated. Thus, there is a possible pathway to quantitative dedoping of the polymer film.

EXPERIMENTAL SECTION

Materials. P3HT (Plextronics, MW = 54−75 kDa, 99.995% trace metals basis) was purchased from Sigma-Aldrich. F4TCNQ was purchased from TCI (98+%). PBTTT-C12 was purchased from Sigma-Aldrich and purified by fractionation into octane followed by centrifugation before reported experiments. PFB was donated by Cambridge Display Technologies. Amines were purchased from VWR; other solvents were purchased from Sigma-Aldrich. Deuterated solvents for NMR were purchased from Cambridge Isotopes.

Thin Film Preparation. One-inch glass substrates (Fisher Scientific) were cleaned by sequential sonication steps in acetone, 10% Mucasol:DI water, and DI water, blown dry with compressed nitrogen, and UV−ozone treated for 30 min before use. P3HT (10 mg/mL, chlorobenzene (CB)) solutions were heated to 60 °C and left to dissolve overnight. F4TCNQ solutions (0.1 mg/mL, acetonitrile) were prepared at room temperature. All F4TCNQ solutions were stored in amber bottles to prevent degradation.[26]

Thin films of P3HT were spin-coated from 60 °C solutions at 1000 rpm until dry. Samples for conductivity and transistor measurements were spin-coated onto silicon chips prepatterned with gold electrodes by photolithography. Films for fluorescence imaging were spin-coated and dedoped (if applicable) before deposition of gold electrodes by thermal evaporation. All films were approximately 50 nm thick, except PFB films which were 60 nm thick, as measured by profilimeter (Dektak 150). Dedoping was performed by soaking doped films in 6 mL of the solutions specified in the text, and then removing the films and allowing them to dry. No additional wash steps were performed unless otherwise specified. All sample preparation and dedoping was performed in a nitrogen glovebox (<3 ppm of H_2O, O_2) equipped with a molecular sieve solvent trap.

Characterization. UV−vis spectra were collected on a PerkinElmer Lambda 750 spectrometer in quartz cuvettes (Thorlabs 10 mm path length and Starna cells, 1 mm path length). All spectra were obtained promptly after addition of the amine. Fluorescence spectra were collected using a Cary Eclipse Fluorimeter, using 540 nm excitation for P3HT and PBTTT, and 350 nm for PFB. Fluorescence imaging was performed on a Zeiss LSM 700 using 488 nm excitation; films were sealed under nitrogen during imaging. Conductivity and transistor measurements were taken using Keithley 2420 source meters connected to a home-built probe station in a nitrogen glovebox. Conductivity measurements were taken in a two bar geometry, by measuring the differential change in voltage with respect to applied current at several different source currents. Transistor measurements were obtained as described previously.[18] NMR spectra were collected on Bruker spectrometers (400, 600, and 800 MHz). Chemical shifts were referenced to residual solvent peaks.[36] Cyclic voltammetry (CV) experiments were performed in argon-purged solutions of acetonitrile, with F4TCNQ:amine and TBAPF6 concentrations of 1 mM and 0.1 M, respectively. All CV experiments were performed using a PC-interfaced BASi Epsilon-EC instrument equipped with a platinum button working electrode (1.6 mm diameter), a stainless steel coil counter electrode, and a Ag/AgCl reference electrode.

RESULTS AND DISCUSSION

F4TCNQ−Amine Reactions. As would be expected given their extreme electrophilicity, TCNQs are susceptible to reaction with nucleophiles such as amines. In fact, the original publication detailing the synthesis of TCNQ[37] was accompanied by two other papers. One detailed the charge transfer complexes formed by TCNQ, helping to launch the field of organic electronics.[38] The other described more than 20

DOI: 10.1021/acs.chemmater.6b04880
Chem. Mater. 2017, 29, 832−841

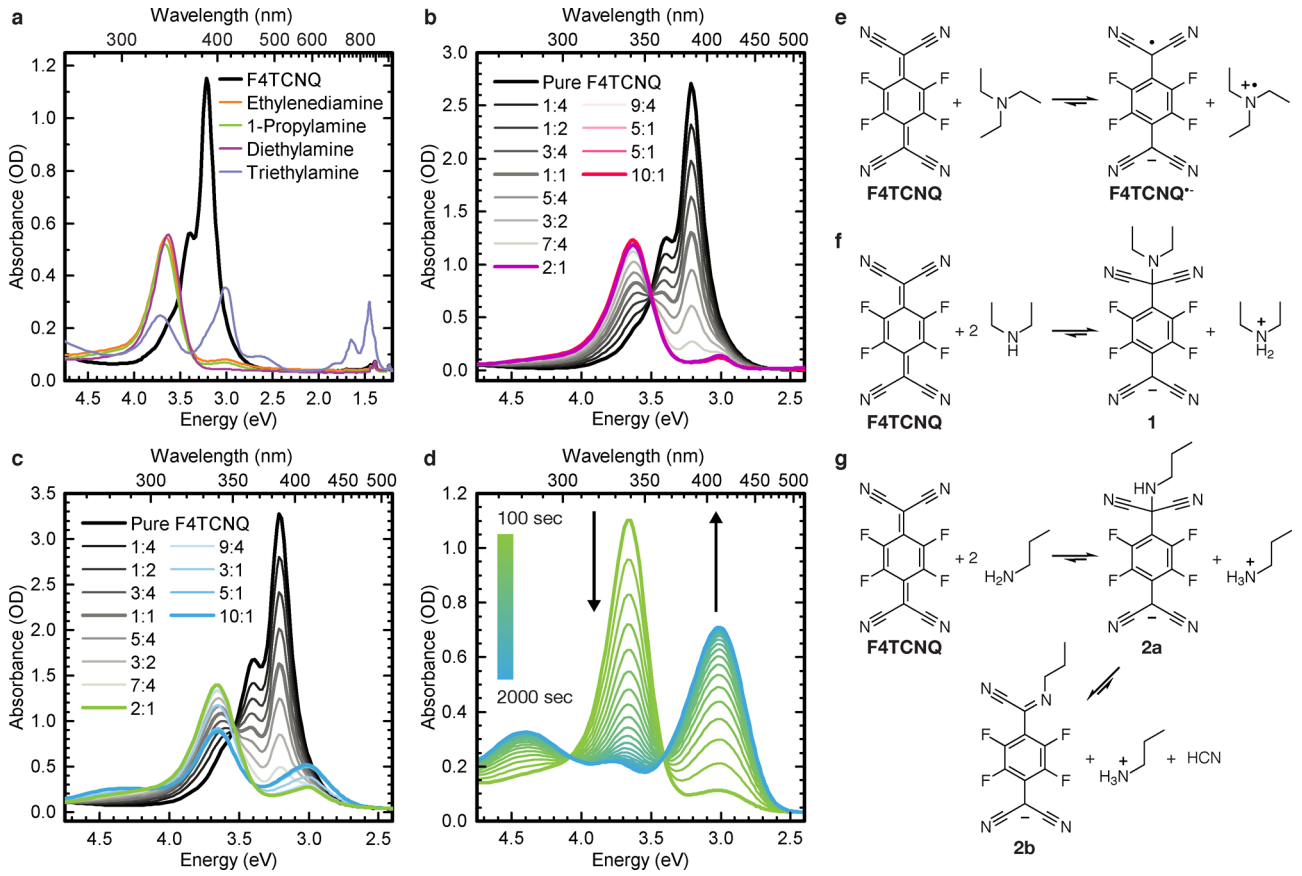

Figure 2. Reactions of 1°, 2°, and 3° amines with F4TCNQ. (a) UV−vis spectra of F4TCNQ (20 μmolar, AN), neat and mixed with amines at 50:1 amine:dopant mole ratio. (b) UV−vis spectra of F4TCNQ (40 μmolar AN), titrated with diethylamine (DEA) at various DEA:F4TCNQ mole ratios. (c) UV−vis spectra of F4TCNQ (50 μmolar, AN), titrated with 1-propylamine (PA) at various PA:F4TCNQ mole ratios. A secondary reaction is clearly visible by the reduction in absorption at 3.7 eV and increased absorption at 3.0 eV at high PA:F4TCNQ ratios. (d) Time dependent UV−vis spectra of F4TCNQ-PA secondary reaction. 10% (v/v) PA was added to a F4TCNQ solution (40 μmolar, AN) immediately before the start of the first scan. Each subsequent scan occurred in 100 s intervals after the initial addition of PA. (e−g) Reaction schemes for F4TCNQ with triethylamine (TEA) (e), DEA (f), and PA (g).

different structures formed by the reaction of various amines with TCNQ.[39]

In this study, we selected three amines: one primary (1-propylamine (PA)), one secondary (diethylamine (DEA)), and one tertiary (triethylamine (TEA)), to study dedoping effectiveness. Figure 2a shows UV−vis spectra of an F4TCNQ solution in acetonitrile (AN), alone and mixed with a 50:1 molar excess of each amine. A spectrum of F4TCNQ with ethylenediamine, which was previously shown to dedope P3HT:F4TCNQ films,[18] is also included. The large excess of amine was used to simulate realistic dedoping conditions, where a thin film containing relatively little F4TCNQ would be treated with a bath of dedoping solution. In all four of the product spectra the neutral F4TCNQ absorption at 390 nm is absent, indicating that the reactions proceed in quantitative yield. The primary and secondary amines all show show similar product absorption peaks at about 3.7 eV (340 nm), while the tertiary amine (TEA) shows absorption bands corresponding to the radical anion,[40] indicative of the reaction shown in Figure 2e. Salts of tertiary amines including TEA:TCNQ have been studied extensively[41,42] and have not been observed to involve covalent bonds between the amine and TCNQ, consistent with our observations in TEA:F4TCNQ. Assuming TEA is a stronger donor than P3HT, we expect that it should function as a competitive dedoping agent.

Although previous studies have indicated that primary and secondary amines do react with TCNQ, the products formed appear to depend on solvent polarity, pH, and amine concentration. To determine the stoichiometry of the reaction, we collected UV−vis spectra of an F4TCNQ solution in AN titrated with DEA and PA. In both cases, UV−vis indicates the reaction proceeds quantitatively within seconds even in dilute (40 μmolar) solutions, so reaction kinetics could not be obtained.

Titration spectra for DEA:F4TCNQ are shown in Figure 2b. The reaction requires two equivalents of DEA to proceed to completion, and at a 1:1 ratio the spectra shows that half of the F4TCNQ is unreacted. This observation is inconsistent with with the previously observed elimination of cyanide to give an aminotricyanoquinodimethane or second substitution yielding diaminodicyanoquinodimethane.[35,39,43] Instead, as shown in Figure 2f, the second equivalent of DEA allows the product **1** to rapidly deprotonate, forming an ion pair. This structure was validated using NMR spectroscopy and cyclic voltammetry (see Supporting Information Sections 1 and 3) confirming that the reaction halts before elimination of −HCN to form the quinone, as has been reported under other conditions.[35,39,43]

DOI: 10.1021/acs.chemmater.6b04880
Chem. Mater. 2017, 29, 832−841

Figure 2c shows the titration spectra for PA:F4TCNQ. Up to a 2:1 PA:F4TCNQ ratio, the spectra are essentially identical to DEA:F4TCNQ and lead to the formation of product **2a**. However, as additional amine is added, the product absorption at 3.7 eV begins to decrease and a new peak at 3.0 eV grows in. Time dependent UV−vis, shown in Figure 2d, reveals the kinetics of this reaction. Each scan is 100 s long. Immediately before the start of the first scan (green) a very large excess (10% v/v) of PA was added to the F4TCNQ solution (40 μmolar, AN), and as a result the first scan shows the spectrum of product **2a**. Over the next 2000 s product **2a** is converted into the second product (**2b**) shown in Figure 2c. The reaction is slower at lower PA concentrations, permitting measurement of the NMR spectra of both the intermediate and the final products. Figure 2g shows the reaction scheme, and Supporting Information Section 2 shows the NMR spectra. Product **2a** is nearly identical to **1** in both UV−vis and NMR spectroscopy, so its assignment was straightforward. The elimination of −HCN to form the imidoyl cyanide, product **2b**, is facilitated by increasing amine concentrations. As with **1**, CV and NMR both indicate that **2b** is a benzylic anion and not a quinone (see Supporting Information Section 3).

During reactive dedoping (Figure 1c−f), the amine initially reduces the doped polymer, forming amine and F4TCNQ radical ions. These ions are not themselves reactive but exist in equilibrium with the neutral species that can then react as shown in Figure 2f,g. To verify that these reactions occur during reactive dedoping, we collected UV−vis spectra of P3HT:F4TCNQ films immersed in AN and AN with varying concentrations of DEA. Figure 3a shows spectra taken through both the film and the solvent, while Figure 3b shows spectra taken with the cuvette rotated 90° so that only the solvent is visible. Figure 3a also shows a P3HT:F4TCNQ film (doped approximately 8 mol %) before immersion.

Exposure to pure AN allows some neutral F4TCNQ to dissolve, as indicated by the absorption at 390 nm in both plots. As expected, dissolution of F4TCNQ results in a reduction in doping level, indicated by an increase in the neutral P3HT $\pi-\pi^*$ absorption (520 nm) and decreases in the P3HT+ polaron band (broad feature 600−900 nm) and $F4TCNQ^{\bullet-}$ bands (750 and 860 nm) relative to the initial doped film. However, when the solution contains DEA, the solution-only spectra (Figure 3b) instead show an absorption feature identical that of product **1**, and the neutral F4TCNQ absorption is no longer visible. The film + solution spectra (Figure 3a) additionally show a strong decrease in film doping level. As the intensity of the reaction product absorption is similar in both plots, we conclude that **1** is highly soluble, and little remains in the film. This is corroborated by UV−vis−NIR spectra of films dedoped with PA (see supporting information Figure S22) which match those of as-cast films. Together, these observations indicate that the reactions shown in Figure 2f,g result in dedoping and removal of F4TCNQ from P3HT films by the mechanism shown in Figure 1.

Very little $F4TCNQ^{\bullet-}$ is observed in the pure AN (Figure 3b, inset) due to the lack of a soluble counterion. However, in the solutions containing low DEA concentrations there is an increase in $F4TCNQ^{\bullet-}$ absorption in solution due to the formation of stable radical ion pairs, analogous to those observed between TEA and F4TCNQ (Figure 2e). Since these $F4TCNQ^{\bullet-}$ ions can only react with DEA or PA through their neutral state, the effective reaction rate is slowed by competition between reactive and competitive dedoping

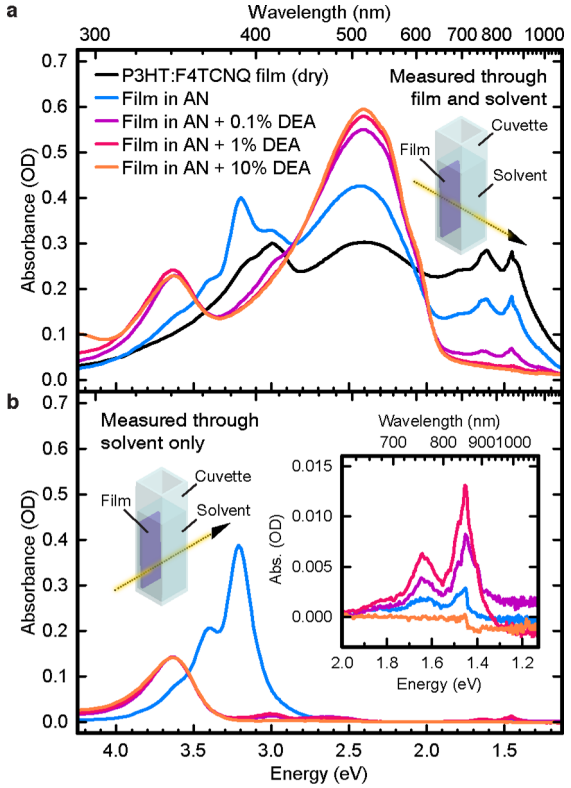

Figure 3. In situ UV−vis spectroscopy of reactive dedoping. (a) Spectra of P3HT:F4TCNQ films dry before immersion, immersed in a cuvette containing AN, and immersed in AN solutions containing varying amounts of DEA. (b) Spectra of the same samples rotated 90° to measure the solvent only. Inset shows $F4TCNQ^{\bullet-}$ absorption. Solution spectra were collected after 5 min of immersion; film + solution spectra were collected after 7 min of immersion.

mechanisms. As a consequence, the dedoping rate is controlled not only by the direct reaction rate of donor and dopant but also by the equilibrium between the ionized and neutral states of the donor and dopant molecules. By increasing the DEA concentration, the forward reaction rate of F4TCNQ and DEA to **1** is increased, resulting in more rapid dedoping. This effect is visible in Figure 3a as a decrease in film doping level with increasing DEA concentration and in Figure 3b as elimination of $F4TCNQ^{\bullet-}$ absorption in solution at 10% DEA. A similar trend is visible in the film fluorescence intensity, shown in Figure S20. Additionally, because the dedoping rate is controlled by the equilibrium between neutral and ionized states of F4TCNQ, we would expect reactive dedoping to occur more quickly in less polar solvents, which shift the equilibrium in favor of the neutral species.

Quantifying Dedoping. Mobile polarons are efficient fluorescence quenchers.[8,44] As a result, fluorescence intensity is highly sensitive to the density of mobile charges (p_{free}) and therefore doping level, allowing for simple detection of residual dopants. In these measurements we use sequential doping from an orthogonal solvent[18,19,45] to separate the effects of additional dopants from impurity levels in the initial polymer film coating. This also allows us to measure the fluorescence intensity of each film before doping as well as after dedoping, controlling for sample-to-sample variation in fluorescence intensity (e.g., from thickness variations).[18] In the following experiments, all films are sequentially doped from an F4TCNQ/AN solution to achieve a doping level of approximately 3.7 mol %.[19] After

DOI: 10.1021/acs.chemmater.6b04880
Chem. Mater. 2017, 29, 832−841

doping, each film is rinsed with CB to allow F4TCNQ to intercalate into the P3HT crystallites.[19] Finally, the films are dedoped by by immersion in a 10% amine solution in a polar carrier solvent which does not dissolve the polymer. See Supporting Information Section 5 for additional information on optimization of dedoping conditions.

Figure 4a shows the integrated fluorescence intensity after dedoping as a function of bath composition and time. As expected, the competitive donor TEA does not fully dedope the film, with fluorescence intensity leveling off at approximately 60% of as-cast emission intensity after a 30 min exposure. The reactive dedoping agents perform much better: DEA:acetone reaches 96% fluorescence recovery after 2 h and 100% after 24 h. Remarkably, dedoping with PA allows for fluorescence recovery of greater than 100%: PA:acetone reaches 124% of as-cast fluorescence intensity after a 2 h exposure. Switching the carrier solvent to cyclohexanone, which is less polar and is also expected to swell P3HT more effectively, increases both the ultimate fluorescence intensity and rate of fluorescence recovery. Figure S19 shows UV−vis spectra of product **2b** formed in cyclohexanone, which indicates that the reaction products formed in cyclohexanone solutions are the same as those formed in AN solutions.

Figure 4b shows fluorescence spectra of a P3HT film as-cast, doped, and dedoped by immersion in a 9:1 cyclohexanone:PA solution for 5 s, 1 min, and 10 min at room temperature. The extremely rapid recovery of fluorescence—110% of as-cast after only a 5 s immersion in an amine solution—indicates that dedoping steps could easily be incorporated into roll-to-roll processing methods. UV−vis spectra of P3HT films dedoped with PA in acetone and cyclohexanone (Figure S22) do not show any changes to vibronic structure after dedoping, indicating that this increase in fluorescence intensity cannot be explained by a reduction in film crystallinity. However, significant increases in P3HT fluorescence have been observed previously after treatment with strong reducing agents or n-type dopants, such as $LiAlH_4$ or cobaltacene, to passivate defect sites.[8,46,47] We will demonstrate in Figure 6 that passivation of intrinsic doping is responsible for the increased film fluorescence observed here.

In previous work,[18] we found that the electrical properties of P3HT films, as measured by field effect transistor (FET) characteristics, could be quantitatively recovered after dedoping. However, in that work, when the devices were dedoped under conditions that fully recovered as-cast film fluorescence, we observed a decrease in hole mobility which did not fully recover after annealing. Alternatively, by reducing the dedoping time we previously recovered as-cast electrical characteristics, but could not simultaneously fully recover the initial fluorescence.[18] No such compromise is required under the optimized conditions described here. Figure 4c shows field effect transistor (FET) transfer curves for a single P3HT device as-cast, after doping, after dedoping with 10% PA:cyclohexanone, and after annealing at 150 °C for 20 min. The as-cast device shows good transfer characteristics ($\log(I_{sd})$, right axis) and a hole mobility of 2×10^{-2} cm^2 V^{-1} s^{-1} obtained from the slope of $I_{sd}^{1/2}$ (left axis). After doping, the source−drain current increases significantly and the device loses all switching capability. This behavior is expected since the density of polarons capacitively accessible by field effect is orders of magnitude lower than the density of doping-induced polarons. Dedoping with 10% PA:cyclohexanone for 15 min recovers switching characteristics but results in a slight decrease in charge carrier mobility. This effect may result from increased trap density due to reduced trap filling,[48] extended solvent exposure time, or residual solvent remaining in the film.[18]

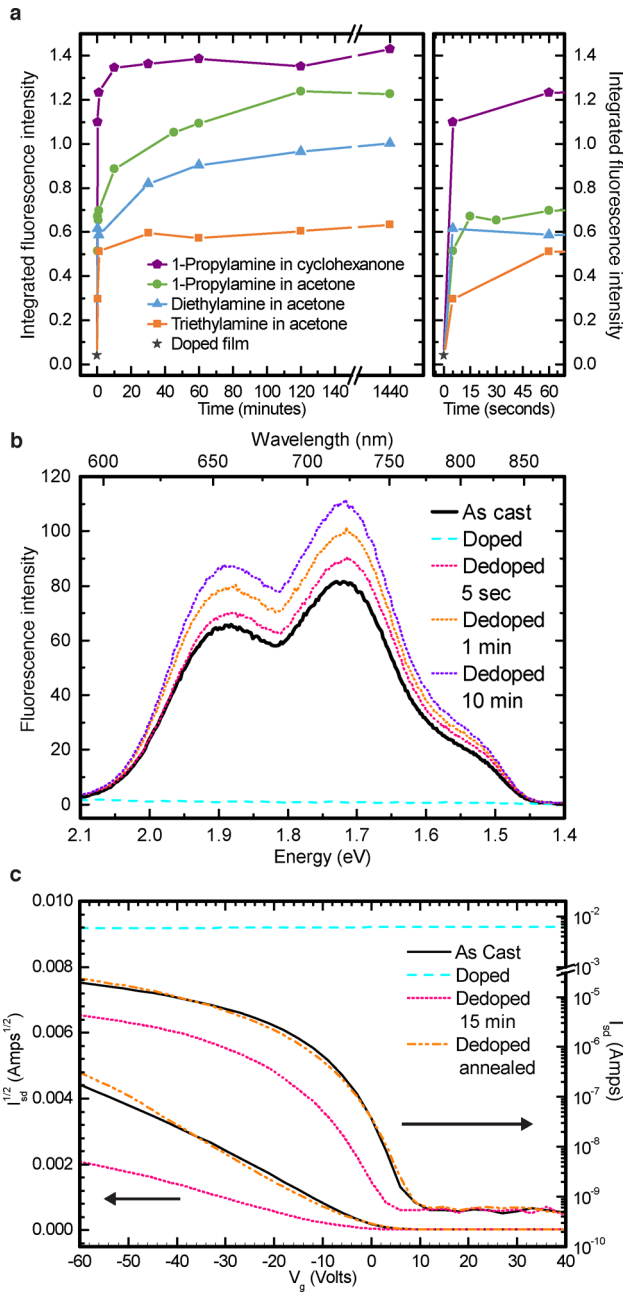

Figure 4. Dedoping kinetics. (a) Integrated fluorescence intensity of dedoped P3HT films as a function of time and dedoping solution. The panel to the right shows an enlarged view of the short time data. For each data point, the dedoped fluorescence intensity is normalized by the as-cast fluorescence intensity of the same film. Before dedoping, doped films show nearly zero fluorescence intensity, as indicated by the black star. Dedoping solutions are 10% amine by volume. (b) Fluorescence spectra of P3HT films as-cast, doped, and dedoped with 10% PA in cyclohexanone for varying times. As in (a), all spectra are normalized by the integrated as-cast fluorescence intensity. (c) Field effect transistor (FET) transfer curves of a single device (50 μm length, 2 mm width) as-cast, doped, dedoped (10% PA in cyclohexanone), and annealed at 150° for 20 min. Right axis shows I_{sd} plotted on a log scale; the same data is replotted on the left axis as $I_{sd}^{1/2}$ on a linear scale, to show carrier mobility. Note that off current is noise limited.

DOI: 10.1021/acs.chemmater.6b04880
Chem. Mater. 2017, 29, 832−841

However, after annealing at 150° for 20 min, mobility recovers to 4×10^{-2} cm^2 V^{-1} s^{-1}, which is higher than that of the as-cast device. Together, the results of Figure 4 show that dedoping with 10% PA in cyclohexanone allows for simultaneous recovery of the intrinsic optical and electrical characteristics of P3HT with properties superior to as-cast films.

We were unable to directly determine the concentration of residual F4TCNQ–amine products in dedoped films. To determine if such products could act as fluorescence quenchers, we measured the HOMO and LUMO energy levels relative to P3HT by cyclic voltammetry of **1**, **2a**, and **2b** (Supporting Information Section 3). For all three compounds, a quasireversible oxidation was observed near 900 mV with respect to the Ag/AgCl reference electrode. These values were converted to vacuum-referenced energies using $E_{HOMO} = e(V_{ox} + V_{ref})$, where e is the elementary charge, V_{ox} is the observed oxidation potential, and V_{ref} is the reference electrode potential (−4.72 V for Ag/AgCl). The resulting HOMO energies are shown in Figure 5, along with those for P3HT.[49] Note that

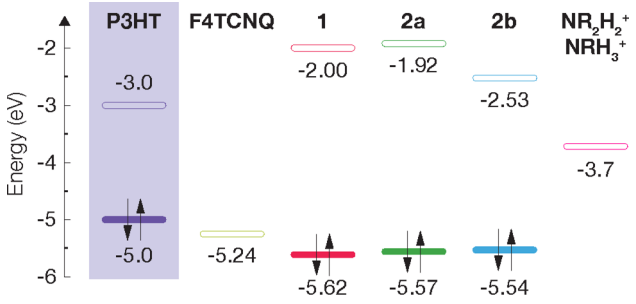

Figure 5. Energy levels of P3HT, F4TCNQ, and F4TCNQ–amine products obtained from CV and UV–vis spectroscopy. Filled bars indicate HOMO levels; unfilled bars indicate LUMO levels. See Supporting Information Section 3 for CV data.

because the CV data showed only quasireversible behavior, it is not possible to account for the oxidation overpotential; as a result, the true HOMO energies may be slightly higher than calculated. Negative potential scans of **1** and **2b** revealed a second quasireversible reduction near −1000 mV in both samples, which we attribute to reduction of the ammonium counterions. No other reductions were visible within the accessible voltage range (up to −2000 mV), indicating that the LUMO energy of **1** and **2b** must be less than 2.7 eV. Negative potential scans of **2a** were not collected but are expected to be similar to those of **1**. To estimate the LUMO energy of each product, we subtracted the optical absorption maximum (in eV) from the CV-derived HOMO energies, shown in Figure 5. In all three cases, both the HOMO and the LUMO energies lie well outside of the P3HT band gap, indicating that these molecules should not quench P3HT excitons or act as trap sites for holes or electrons. However, it appears that the ammonium cations should be capable of accepting an electron from P3HT*, quenching P3HT fluorescence.

The fact that greater than as-cast fluorescence intensities are consistently observed in dedoped films in spite of the possible presence of ammonium cations indicates that the concentration of these cations (and corresponding **2a**/**2b** anions) must be significantly lower than the density of intrinsic fluorescence quenching defects in as-cast films. The low concentration of **2a**/**2b** in dedoped films is likely due to the product's ionic character. When dried, **2b** is highly soluble in polar solvents such as AN and cyclohexanone, but completely insoluble in low dielectric solvents such as toluene, as expected for a salt. The dielectric constant of most conductive polymers is quite low (typically around 3), so we do not expect significant solubility of products **1**, **2a**, or **2b** in the polymer.

It is likely that by switching to a less basic donor, the neutral, protonated forms of the products shown in Figure 2 could be obtained, as was the case with the F4TCNQ–THF photoreaction product.[26] This product had an extremely large optical bandgap (>6 eV) and was not a quinone, so it would not be expected to quench fluorescence or interact electrically with most polymers. However, the protonated states of these molecules would likely be more soluble in the polymers than the salts shown in Figure 2.

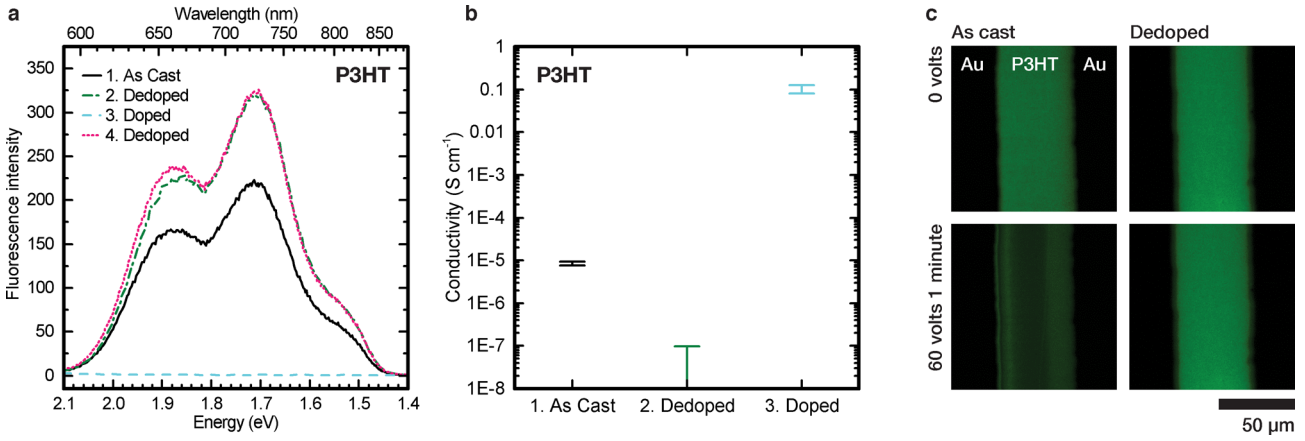

Figure 6. PA:cyclohexanone treatment dedopes as-cast films. (a) Fluorescence spectra of an as-cast P3HT film (black), the same film after 15 min dedoping treatment (10%PA in cyclohexanone) (green dotted-dashed), after a sequential doping treatment with F4TCNQ (0.1 mg/mL AN) (cyan dashed), and after a second 15 min dedoping treatment (10% PA in cyclohexanone) (red dotted). (b) Two-bar conductivity measurements after steps 1–3 in (a) (same film). (c) Fluorescence laser scanning confocal microscopy (LSCM) images of as-cast and dedoped (10%PA in cyclohexanone) films with evaporated gold electrodes. Upper images show the films before voltage was applied; lower images show films after application of 60 V for 1 min. Samples were sealed in a nitrogen atmosphere during imaging.

DOI: 10.1021/acs.chemmater.6b04880
Chem. Mater. 2017, 29, 832–841

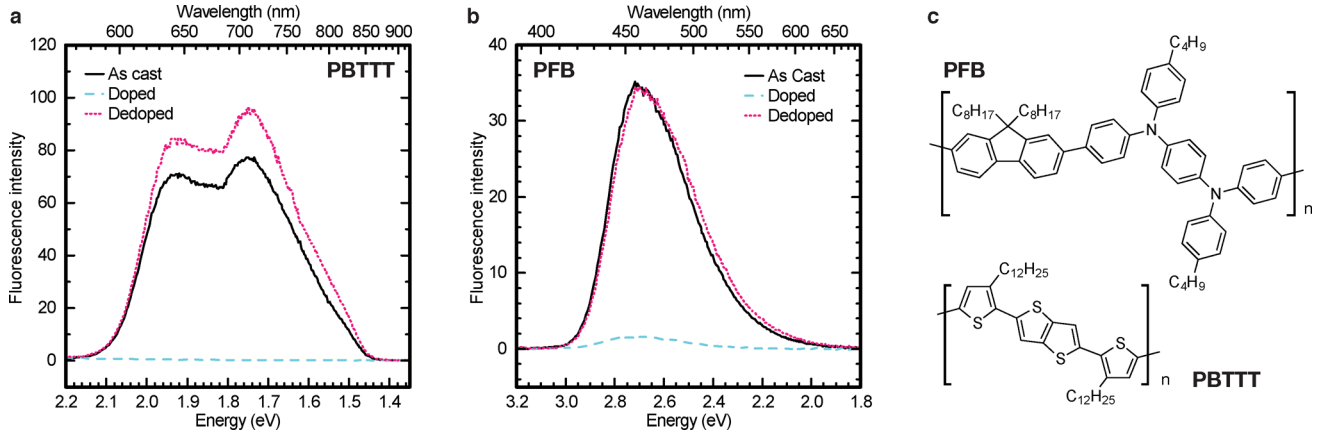

Figure 7. Dedoping other polymers. (a) Fluorescence spectra of a single PBTTT film as-cast, after doping with F4TCNQ (0.1 mg/mL AN), and after dedoping (10% DEA in acetone, 120 min). (b) Fluorescence spectra of a single PFB film as-cast, after doping with F4TCNQ (0.1 mg/mL AN), and after dedoping (10% PA in acetone, 120 min). (c) Chemical structures of PBTTT and PFB.

EFFECT OF PA ON INTRINSIC DEFECTS

To determine whether one of the dedoping products or PA itself was responsible for the increase in fluorescence intensity seen in Figure 4b, we repeated the dope–dedope experiment but inserted an additional dedoping step *before* doping the film. As shown in Figure 6a, this initial dedoping step does indeed result in the same increase in film fluorescence. Since mobile charge carriers are known to quench excitions much more efficiently than bound charges,[8] this observation suggests that PA treatment is acting to reduce the density of mobile charges. Conductivity measurements (Figure 6b) confirm this. Exposure to 10% PA:cyclohexanone for 10 min results in at least a 2 orders of magnitude reduction in conductivity (the exact conductivity of the film after dedoping could not be determined). The conductivity decrease with PA treatment is direct evidence of a reduction in free charge carriers.

Figure 6c shows fluorescence microscopy images of P3HT films in field effect geometry (P3HT fluorescence is false colored green, black regions are gold electrodes). For as-cast devices, application of voltage forces some of the bound polaron–defect pairs to separate, increasing the free carrier density and resulting in increased fluorescence quenching. This effect has been previously observed in isolated chains of the conjugated polymer MEH-PPV (poly[2-methoxy-5-(2-ethylhexyloxy)-1,4-phenylenevinylene]), where application of an electric field caused the fluorescence of isolated chains to blink off.[50] The authors attributed these effects to field-assisted separation of charged defect pairs. After PA treatment, these bound charge pairs are passivated, resulting in fluorescence images which are unchanged under high applied electric fields.

Interestingly, treating as-cast P3HT films with DEA does not affect fluorescence intensity (see Supporting Information Figure S23). Both PA and DEA have similar pK_a values and so would be expected to perform similarly well as compensating dopants. This observation suggests that PA may be acting to chemically passivate polymer defect sites via a reaction mechanism that is not available to secondary amines. Unfortunately, as other authors have noted,[8,46,47] the low density of the relevant defect sites makes their chemical characterization difficult.

Commercially available conjugated polymer samples vary widely in quality including differences in MW, PDI, and impurity density. Post-treatment of films with amines is a simple method to increase the fluorescence quantum yield and likely improves associated properties (exciton lifetime, etc.) of lower quality samples as well. To illustrate the usefulness of this approach, we repeated the same dope–dedope experiments shown in Figure 4 on a sample of PBTTT which showed relatively low field effect mobilites (see Supporting Information Figure S24 and Table S5). In this material, dedoping with DEA yielded a significant increase in film fluorescence (Figure 7a). DEA treatment has no effect on as-cast P3HT films (Figure S23); therefore, the defects present in this PBTTT sample must be different from those in our P3HT sample. Field effect mobilities remained essentially unchanged after dedoping. These results serve to illustrate that the nature of defect sites varies between different polymers and likely even individual polymer samples.

In contrast, we also performed the same experiment on a very clean sample of PFB, a highly fluorescent blue emitting polymer which can be doped by F4TCNQ,[51] provided to us by Cambridge Display Technologies. This measurement represents a "worst-case scenario" for dedoping, as its fluorescence quantum yield is high and defect density is low, so full recovery of fluorescence intensity should only be possible if the F4TCNQ is quantitatively removed. As seen in Figure 7b, after doping with F4TCNQ and dedoping with PA, dedoped fluorescence was virtually identical to that of as-cast, indicating that the F4TCNQ was quantitatively removed.

The method we describe here achieves results similar to those of the defect engineering approach described by Liang and co-workers.[8,46,47] However, the reducing agents used in these works were $LiAlH_4$[46,47] or cobaltacene,[8] both of which are strongly reactive toward oxygen or water and require more specialized handling procedures.

In summary, we have suggested a mechanism, reactive dedoping, by which it is possible to dedope (as opposed to merely compensation dope) semiconducting polymers. Using P3HT:F4TCNQ as a model system, we have identified a reaction between F4TCNQ and PA which even allows for greater than quantitative recovery of film fluorescence. Once optimized, we found that this process enables fluorescence recovery to at least as-cast levels in less than 5 s at room temperature, allowing for easy integration into roll-to-roll coating processes. Because p-type dopant molecules are by nature strongly electrophilic, they are susceptible to attack by nucleophiles such as amines, while n-type dopants are expected

DOI: 10.1021/acs.chemmater.6b04880
Chem. Mater. 2017, 29, 832–841

to be prone to electrophilic attack. Therefore, reactive dedoping processes should be simple to engineer in a wide range of p- and n-type doped organic semiconductors.

In addition, treatment of undoped films with PA results in increased film fluorescence and a reduction in conductivity, consistent with removal of intrinsic charged defects. Quantitative fluorescence recovery is possible even in low-defect, high fluorescence yield samples such as PFB. The ability to sequentially add and then quantitatively remove dopants, often achieving doping levels at or below that of as-cast films, paves the way for new applications of doping in organic materials, in which not only electrical and optical properties but also physical properties such as solubility can be locally and reversibly controlled. This chemical treatment is a simple and essentially nontoxic solution process that can be used in-line with any solution-processable conjugated polymer, making it a potentially valuable addition to the organic electronics processing toolkit.

■ ASSOCIATED CONTENT

Supporting Information

The Supporting Information is available free of charge on the ACS Publications website at DOI: 10.1021/acs.chemmater.6b04880.

NMR spectra and cyclic voltammetry of **1**, **2a**, and **2b**, additional UV−vis spectra of **1** and **2b**, information on optimization of dedoping conditions, and field-effect transistor measurements of PBTTT (PDF)

■ AUTHOR INFORMATION

Corresponding Author

*E-mail: amoule@ucdavis.edu.

ORCID

Ian E. Jacobs: 0000-0002-1535-4608

Notes

The authors declare no competing financial interest.

■ ACKNOWLEDGMENTS

This research project was supported by the U.S. Department of Energy, Office of Basic Energy Sciences, Division of Materials Sciences and Engineering, under Award No. DE-SC0010419. I.E.J. and J.L. thank the University of California Advanced Solar Technologies Institute (UC Solar) for funding. C.M.-P. gratefully acknowledges PIF-UVa and EB-15 for funding and M. Luz Rodriguez-Mendez for support. We also thank Cambridge Display Technologies for donation of the PFB sample.

■ REFERENCES

(1) Mead, C.; Conway, L. *Introduction to VLSI Systems*; Addison-Wesley: Reading, MA, 1980; Vol. *1080*.

(2) Arias, A. C.; MacKenzie, J. D.; McCulloch, I.; Rivnay, J.; Salleo, A. Materials and Applications for Large Area Electronics: Solution-Based Approaches. *Chem. Rev.* **2010**, *110*, 3−24.

(3) Gelinck, G. H.; et al. Flexible Active-Matrix Displays and Shift Registers Based on Solution-Processed Organic Transistors. *Nat. Mater.* **2004**, *3*, 106−110.

(4) Hammock, M. L.; Chortos, A.; Tee, B. C. K.; Tok, J. B. H.; Bao, Z. 25th Anniversary Article: The Evolution of Electronic Skin (E-Skin): A Brief History, Design Considerations, and Recent Progress. *Adv. Mater.* **2013**, *25*, 5997−6038.

(5) Mazzio, K. A.; Luscombe, C. K. The Future of Organic Photovoltaics. *Chem. Soc. Rev.* **2015**, *44*, 78−90.

(6) Kippelen, B.; Bredas, J. L. Organic Photovoltaics. *Energy Environ. Sci.* **2009**, *2*, 251−261.

(7) Sze, S. M.; Ng, K. K. *Physics of Semiconductor Devices*; John Wiley & Sons: 2006.

(8) Liang, Z.; Gregg, B. A. Compensating Poly(3-hexylthiophene) Reveals Its Doping Density and Its Strong Exciton Quenching by Free Carriers. *Adv. Mater.* **2012**, *24*, 3258−3262.

(9) Pingel, P.; Neher, D. Comprehensive Picture of p-Type Doping of P3HT With the Molecular Acceptor F_4TCNQ. *Phys. Rev. B: Condens. Matter Mater. Phys.* **2013**, *87*, 115209.

(10) Gao, J.; Roehling, J. D.; Li, Y.; Guo, H.; Moule, A. J.; Grey, J. K. The Effect of 2,3,5,6-tetrafluoro-7,7,8,8-tetracyanoquinodimethane Charge Transfer Dopants on the Conformation and Aggregation of Poly(3-hexylthiophene). *J. Mater. Chem. C* **2013**, *1*, 5638−5646.

(11) Gao, J.; Niles, E. T.; Grey, J. K. Aggregates Promote Efficient Charge Transfer Doping of Poly(3-hexylthiophene). *J. Phys. Chem. Lett.* **2013**, *4*, 2953−2957.

(12) Duong, D. T.; Wang, C.; Antono, E.; Toney, M. F.; Salleo, A. The Chemical and Structural Origin of Efficient p-type Doping in P3HT. *Org. Electron.* **2013**, *14*, 1330−1336.

(13) Duong, D. T.; Phan, H.; Hanifi, D.; Jo, P. S.; Nguyen, T.-Q.; Salleo, A. Direct Observation of Doping Sites in Temperature-Controlled, p-Doped P3HT Thin Films by Conducting Atomic Force Microscopy. *Adv. Mater.* **2014**, *26*, 6069−6073.

(14) Gao, J.; Stein, B. W.; Thomas, A. K.; Garcia, J. A.; Yang, J.; Kirk, M. L.; Grey, J. K. Enhanced Charge Transfer Doping Efficiency in J-Aggregate Poly(3-hexylthiophene) Nanofibers. *J. Phys. Chem. C* **2015**, *119*, 16396−16402.

(15) Wang, C.; Duong, D. T.; Vandewal, K.; Rivnay, J.; Salleo, A. Optical Measurement of Doping Efficiency in Poly(3-hexylthiophene) Solutions and Thin Films. *Phys. Rev. B: Condens. Matter Mater. Phys.* **2015**, *91*, 085205.

(16) Li, J.; Zhang, G.; Holm, D. M.; Jacobs, I. E.; Yin, B.; Stroeve, P.; Mascal, M.; Moulé, A. J. Introducing Solubility Control for Improved Organic P-Type Dopants. *Chem. Mater.* **2015**, *27*, 5765−5774.

(17) Li, J.; Rochester, C. W.; Jacobs, I. E.; Friedrich, S.; Stroeve, P.; Riede, M.; Moule, A. J. Measurement of Small Molecular Dopant F4TCNQ and C60F36 Diffusion in Organic Bilayer Architectures. *ACS Appl. Mater. Interfaces* **2015**, *7*, 28420−28428.

(18) Jacobs, I. E.; Li, J.; Burg, S. L.; Bilsky, D. J.; Rotondo, B. T.; Augustine, M. P.; Stroeve, P.; Moulé, A. J. Reversible Optical Control of Conjugated Polymer Solubility with Sub-micrometer Resolution. *ACS Nano* **2015**, *9*, 1905−1912.

(19) Jacobs, I. E.; Aasen, E. W.; Oliveira, J. L.; Fonseca, T. N.; Roehling, J. D.; Li, J.; Zhang, G.; Augustine, M. P.; Mascal, M.; Moule, A. J. Comparison of Solution-Mixed and Sequentially Processed P3HT:F4TCNQ Films: Effect of Doping-Induced Aggregation on Film Morphology. *J. Mater. Chem. C* **2016**, *4*, 3454−3466.

(20) Kao, C. Y.; Lee, B.; Wielunski, L. S.; Heeney, M.; McCulloch, I.; Garfunkel, E.; Feldman, L. C.; Podzorov, V. Doping of Conjugated Polythiophenes with Alkyl Silanes. *Adv. Funct. Mater.* **2009**, *19*, 1906−1911.

(21) Chiang, J.-C.; MacDiarmid, A. G. 'Polyaniline': Protonic Acid Doping of the Emeraldine Form to the Metallic Regime. *Synth. Met.* **1986**, *13*, 193−205.

(22) Dominis, A. J.; Spinks, G. M.; Kane-Maguire, L. A. P.; Wallace, G. G. A De-Doping/Re-Doping Study of Organic Soluble Polyaniline. *Synth. Met.* **2002**, *129*, 165−172.

(23) MacDiarmid, A. G.; Epstein, A. J. Secondary Doping in Polyaniline. *Synth. Met.* **1995**, *69*, 85−92.

(24) Cao, Y.; Smith, P.; Heeger, A. J. Counter-Ion Induced Processibility of Conducting Polyaniline. *Synth. Met.* **1993**, *57*, 3514−3519.

(25) Jacobs, I. E.; Aasen, E. W.; Nowak, D.; Li, J.; Morrison, W.; Roehling, J. D.; Augustine, M. P.; Moulé, A. J. Direct-Write Optical Patterning of P3HT Films Beyond the Diffraction Limit. *Adv. Mater.* **2017**, *29*, 1603221.

(26) Fuzell, J.; Jacobs, I. E.; Ackling, S.; Harrelson, T. F.; Huang, D. M.; Larsen, D.; Moulé, A. J. Optical Dedoping Mechanism for P3HT:F4TCNQ Mixtures. *J. Phys. Chem. Lett.* **2016**, *7*, 4297−4303.
(27) Winkler, S.; Amsalem, P.; Frisch, J.; Oehzelt, M.; Heimel, G.; Koch, N. Probing the Energy Levels in Hole-Doped Molecular Semiconductors. *Mater. Horiz.* **2015**, *2*, 427−433.
(28) Shirakawa, H.; Louis, E. J.; MacDiarmid, A. G.; Chiang, C. K.; Heeger, A. J. Synthesis of Electrically Conducting Organic Polymers: Halogen Derivatives of Polyacetylene, (CH). *J. Chem. Soc., Chem. Commun.* **1977**, 578−580.
(29) Jen, K.-Y.; Miller, G. G.; Elsenbaumer, R. L. Highly Conducting, Soluble, and Environmentally-Stable Poly(3-alkylthiophenes). *J. Chem. Soc., Chem. Commun.* **1986**, 1346−1347.
(30) Heeger, A. J.; Kivelson, S.; Schrieffer, J. R.; Su, W. P. Solitons in Conducting Polymers. *Rev. Mod. Phys.* **1988**, *60*, 781−850.
(31) Salzmann, I.; Heimel, G.; Duhm, S.; Oehzelt, M.; Pingel, P.; George, B. M.; Schnegg, A.; Lips, K.; Blum, R.-P.; Vollmer, A.; Koch, N. Intermolecular Hybridization Governs Molecular Electrical Doping. *Phys. Rev. Lett.* **2012**, *108*, 035502.
(32) Méndez, H.; Heimel, G.; Opitz, A.; Sauer, K.; Barkowski, P.; Oehzelt, M.; Soeda, J.; Okamoto, T.; Takeya, J.; Arlin, J.-B.; Balandier, J.-Y.; Geerts, Y.; Koch, N.; Salzmann, I. Doping of Organic Semiconductors: Impact of Dopant Strength and Electronic Coupling. *Angew. Chem., Int. Ed.* **2013**, *52*, 7751−7755.
(33) Salzmann, I.; Heimel, G.; Oehzelt, M.; Winkler, S.; Koch, N. Molecular Electrical Doping of Organic Semiconductors: Fundamental Mechanisms and Emerging Dopant Design Rules. *Acc. Chem. Res.* **2016**, *49*, 370−378.
(34) Heimel, G. The Optical Signature of Charges in Conjugated Polymers. *ACS Cent. Sci.* **2016**, *2*, 309−315.
(35) El Seoud, O. A.; Ribeiro, F. P.; Martins, A.; Brotero, P. P. Kinetics of the Reaction of Alkylamines with 7,7,8,8-Tetracyanoquinodimethane (TCNQ) in Organic Solvents. *J. Org. Chem.* **1985**, *50*, 5099−5102.
(36) Gottlieb, H. E.; Kotlyar, V.; Nudelman, A. NMR Chemical Shifts of Common Laboratory Solvents as Trace Impurities. *J. Org. Chem.* **1997**, *62*, 7512−7515.
(37) Acker, D. S.; Hertler, W. R. Substituted Quinodimethans. I. Preparation and Chemistry of 7,7,8,8-Tetracyanoquinodimethan. *J. Am. Chem. Soc.* **1962**, *84*, 3370−3374.
(38) Melby, L. R.; Harder, R. J.; Hertler, W. R.; Mahler, W.; Benson, R. E.; Mochel, W. E. Substituted Quinodimethans. II. Anion-radical Derivatives and Complexes of 7,7,8,8-Tetracyanoquinodimethan. *J. Am. Chem. Soc.* **1962**, *84*, 3374−3387.
(39) Hertler, W. R.; Hartzler, H. D.; Acker, D. S.; Benson, R. E. Substituted Quinodimethans. III. Displacement Reactions of 7,7,8,8-Tetracyanoquinodimethan. *J. Am. Chem. Soc.* **1962**, *84*, 3387−3393.
(40) Jonkman, H. T.; Kommandeur, J. The UV Spectra and their Calculation of TCNQ and its Mono- and Di-Valent Anion. *Chem. Phys. Lett.* **1972**, *15*, 496−499.
(41) Kepler, R. G.; Bierstedt, P. E.; Merrifield, R. E. Electronic Conduction and Exchange Interaction in a New Class of Conductive Organic Solids. *Phys. Rev. Lett.* **1960**, *5*, 503−504.
(42) Torrance, J. B.; Scott, B. A.; Kaufman, F. B. Optical Properties of Charge Transfer Salts of Tetracyanoquinodimethane (TCNQ). *Solid State Commun.* **1975**, *17*, 1369−1373.
(43) de Caro, D.; Souque, M.; Faulmann, C.; Coppel, Y.; Valade, L.; Fraxedas, J.; Vendier, O.; Courtade, F. Colloidal Solutions of Organic Conductive Nanoparticles. *Langmuir* **2013**, *29*, 8983−8988.
(44) Ferguson, A. J.; Kopidakis, N.; Shaheen, S. E.; Rumbles, G. Quenching of Excitons by Holes in Poly(3-hexylthiophene) Films. *J. Phys. Chem. C* **2008**, *112*, 9865−9871.
(45) Ingram, I. D. V.; Tate, D. J.; Parry, A. V. S.; Sebastian Sprick, R.; Turner, M. L. A Simple Method for Controllable Solution Doping of Complete Polymer Field-Effect Transistors. *Appl. Phys. Lett.* **2014**, *104*, 153304.
(46) Liang, Z.; Nardes, A.; Wang, D.; Berry, J. J.; Gregg, B. A. Defect Engineering in p-Conjugated Polymers. *Chem. Mater.* **2009**, *21*, 4914−4919.
(47) Liang, Z.; Reese, M. O.; Gregg, B. A. Chemically Treating Poly(3-hexylthiophene) Defects to Improve Bulk Heterojunction Photovoltaics. *ACS Appl. Mater. Interfaces* **2011**, *3*, 2042−2050.
(48) Shang, Z.; Heumueller, T.; Prasanna, R.; Burkhard, G. F.; Naab, B. D.; Bao, Z.; McGehee, M. D.; Salleo, A. Trade-Off between Trap Filling, Trap Creation, and Charge Recombination Results in Performance Increase at Ultralow Doping Levels in Bulk Heterojunction Solar Cells. *Adv. Energy Mater.* **2016**, *6*, 1601149.
(49) Johansson, T.; Mammo, W.; Svensson, M.; Andersson, M. R.; Inganas, O. Electrochemical Bandgaps of Substituted Polythiophenes. *J. Mater. Chem.* **2003**, *13*, 1316−1323.
(50) Hania, P. R.; Scheblykin, I. G. Electric Field Induced Quenching of the Fluorescence of a Conjugated Polymer Probed at the Single Molecule Level. *Chem. Phys. Lett.* **2005**, *414*, 127−131.
(51) Yim, K.-H.; Whiting, G. L.; Murphy, C. E.; Halls, J. J. M.; Burroughes, J. H.; Friend, R. H.; Kim, J.-S. Controlling Electrical Properties of Conjugated Polymers via a Solution-Based p-Type Doping. *Adv. Mater.* **2008**, *20*, 3319−3324.

DOI: 10.1021/acs.chemmater.6b04880
Chem. Mater. 2017, 29, 832−841